A Novel Type of ATP Block on a Ca^{2+}-Activated K^+ Channel from Bullfrog Erythrocytes

M. Shindo,* Y. Imai, and Y. Sohma
Department of Physiology, Osaka Medical College, Takatsuki, Osaka 569-8686, Japan

ABSTRACT Using the patch-clamp technique, we have identified an intermediate conductance Ca^{2+}-activated K^+ channel from bullfrog (*Rana catesbeiana*) erythrocytes and have investigated the regulation of channel activity by cytosolic ATP. The channel was highly selective for K^+ over Na^+, gave a linear I-V relationship with symmetrical 117.5 mM K^+ solutions and had a single-channel conductance of 60 pS. Channel activity was dependent on Ca^{2+} concentration ($K_{1/2}$ = 600 nM) but voltage-independent. These basic characteristics are similar to those of human and frog erythrocyte Ca^{2+}-activated K^+ (Gardos) channels previously reported. However, cytoplasmic application of ATP reduced channel activity with block exhibiting a novel bell-shaped concentration dependence. The channel was inhibited most by ~10 μM ATP (P_o reduced to 5% of control) but less blocked by lower and higher concentrations of ATP. Moreover, the novel type of ATP block did not require Mg^{2+}, was independent of PKA or PKC, and was mimicked by a nonhydrolyzable ATP analog, AMP-PNP. This suggests that ATP exerts its effect by direct binding to sites on the channel or associated regulatory proteins, but not by phosphorylation of either of these components.

INTRODUCTION

A wide variety of Ca^{2+}-activated K^+ channels have been identified in many different tissues and these channels play important roles in many cell functions. It is well known that these channels are regulated by membrane voltage and cytosolic calcium (see Latorre et al., 1989; McManus, 1991 for review). In addition to their regulation by voltage and calcium, there is increasing evidence that Ca^{2+}-activated K^+ channels are also regulated by neurotransmitters, hormones, lipids, and nucleotides. (see Toro and Stefani, 1991 for review). In the case of nucleotides, ATP has been shown to regulate the activity of several Ca^{2+}-activated K^+ channels via protein phosphorylation and by other mechanisms (see Levitan, 1994; Hilgemann, 1997 for review). However, the regulatory characteristics and mechanisms involved in the modulation of Ca^{2+}-activated K^+ channels, especially IK- and SK-channels, by ATP are still unclear.

The Gardos channel present in erythrocytes (Hamill, 1983; Grygorcyzk and Schartz, 1983) is now categorized as an $SK_{(Ca)}$ channel (Latorre et al., 1989; McManus, 1991), and underlies the Ca^{2+}-activated K^+ permeability in human erythrocyte treated with glycolytic inhibitors (ATP-depleted cell) (Gardos, 1958). In addition to Ca^{2+} and voltage, it has been reported that the channel was regulated by ATP via cAMP-mediated and nonmediated phosphorylation (Romero et al., 1990; Romero and Rojas, 1992).

In this report, we have identified an intermediate conductance Ca^{2+}-activated K^+ channel on bullfrog erythrocytes using the patch-clamp technique and investigated the regulation of channel activity by intracellular ATP.

MATERIALS AND METHODS

Erythrocyte preparation

Fresh blood was obtained from double-pithed bullfrogs (*Rana catesbeiana*, purchased from Hokusetsu Sangyo, Osaka, Japan) with heparinization. The cells were washed once or twice in the Na^+-rich solutions containing 100 μM Ca^{2+} (see below) and put on a coverslip coated with a cell adhesive (Cell-Tak, Becton Dickinson Labware, Bedford, MA).

Measurement of single-channel activity

Patch-clamp experiments were performed as previously described (Sohma et al. 1996, 1998). Single-channel recordings were obtained from excised, inside-out patches using an Axopatch 200A patch-clamp amplifier (Axon Instruments, Inc., Foster City, CA). Patch pipettes were pulled from borosilicate glass capillaries (GC120F15, Clark Electromedical Instruments, Pangbourne, UK) using a vertical electrode puller (PP-83, Narishige Scientific Instrument Laboratories, Tokyo, Japan) and had resistance of between 7 and 11 MΩ after fire polishing. The coverslip on which erythrocytes were adhered was put in a bath chamber placed on the stage of an inverted microscope (Diaphoto-TMD, Nikon, Tokyo, Japan) mounted on a vibration-isolation table (ORE-1290, Showa Electric Wire and Cable Co., Tokyo, Japan). The pipette was advanced to the cell surface using a three-dimensional hydraulic micromanipulator (MW-3, Narishige Scientific) under direct observation (×400). Giga seal formation (3–7 GΩ) was achieved by application of light suction to the pipette interior, although seals formed spontaneously on rare occasions. After sealing, the inside-out configuration was achieved by withdrawing the pipette tip from the cell. The tissue bath was grounded, and potential difference across excised, inside-out patches (V_m) was referenced to the extracellular face of the membrane. The observed current records were stored on videotapes using a modified digital audio processor for off-line analysis.

The Na^+-rich solution had the following composition: 115 mM NaCl, 2.5 mM KCl, 10 mM HEPES, with various concentration of free Ca^{2+} at pH 7.4. The K^+-rich solution contained: 117.5 mM KCl, 10 mM HEPES,

Received for publication 15 April 1999 and in final form 30 March 2000.

Address reprint requests to Dr. Y. Sohma, Department of Physiology, Osaka Medical College, 2-7 Daigaku-machi, Takatsuki, Osaka 569-8686, Japan. Tel: +81-726-83-1221 ext. 2654; Fax: +81-726-84-6520; E-mail: yoshiros@art.osaka-med.ac.jp.

Dr. Shindo's present address is Yosanoumi Hospital, Miyazu, Kyoto 629-2261, Japan.

0006-3495/00/07/287/11 $2.00

with various concentration of free Ca^{2+} at pH 7.4. A buffer system that contained 2 mM EGTA and variable amounts of $CaCl_2$ was used to stabilize free-Ca^{2+} concentration. The free-Ca^{2+} concentrations in these solutions were calculated using EQCAL program (Biosoft, Cambridge, UK). For the pipette solution, the K^+-rich solution with no $CaCl_2$ and 2 mM EGTA, or with 2 mM Ca^{2+} was used with filtering through a 0.2 μm membrane filter.

In some experiments, 2 mM $MgCl_2$ or 4–400 μM LiCl was added to the bath solution. Sodium adenosine-5′-monophosphate (Na_2AMP, Sigma, St. Louis, MO), sodium adenosine-5′-diphosphate (Na_2ADP, Sigma), sodium adenosine-5′-triphosphate (Na_2ATP, Sigma), magnesium adenosine-5′-triphosphate (MgATP, Sigma) and a non-hydrolyzable ATP analog, 5′-adenylyl imidodiphosphate lithium salt (AMP-PNP, Sigma; approx. 95% purity and containing 4–5.2% lithium) were dissolved in the Na^+-rich solution containing 2 mM $CaCl_2$ and no EGTA and pH was readjusted to 7.4. Because AMP-PNP was added in the form of a lithium salt (4 Li^+ per molecule), we confirmed that addition of 4–400 μM Li^+ (LiCl) did not affect the channel activity significantly (data not shown). This means that Li^+ made little contribution to the inhibitory effect of AMP-PNP. A specific protein kinase A (PKA) inhibitor {*N*-[2-((p-Bromocinnamyl)amino)ethyl]-5-isoquinolinesulfonamide, HCl} (H-89, Calbiochem-Novabiochem, La Jolla, CA), a specific protein kinase C (PKC) inhibitor {2-[1-(3-Dimethylaminopropyl)-^{1}H-indol-3-yl]-3-(^{1}H-indol-3-yl)maleimide, HCl} (Bisindolylmaleimide I, Hydrochloride, Calbiochem-Novabiochem) and an ATP-sensitive K^+ channel inhibitor (Glibenclamide, Sigma) were used in required experiments. H-89 and glibenclamide were dissolved in dimethyl sulfoxide (DMSO, Sigma) and added in the bath solution with a final concentration of 0.1% DMSO, which, alone, did not affect channel activity. All other chemicals were purchased from commercial sources and were of the highest purity available.

We had experimental problems in obtaining and maintaining the giga-seal. Therefore, we used a Ca^{2+} -free pipette solution for obtaining the giga-seal regularly (Hamill, 1983; Christophersen, 1991). We also confirmed that, in some patches with the pipette solution containing 2 mM Ca^{2+}, the ATP block occurred in the same way and pooled the data. For maintaining the giga-seal over a long period, we usually recorded single-channel currents at $V_m = -20$ mV, a small hyperpolarized potential (see Figs. 4–7), and used the data at $V_m = -20$ mV for normalizing the data obtained at other V_m (see Fig. 2 *C*). Note that the channel activity was virtually voltage independent (see Fig. 2 *C*).

All experiments were performed at room temperature (21–23°C) between March and November. It was hard to find channel activity on the untreated erythrocytes during the wintertime (from December to February).

Data analysis

The recorded currents were filtered at 200 or 1 kHz by an 8-pole lowpass Bessel filter (Model LPF902, Frequency Devices, Haverhill, MA) and sampled at 5 kHz by an A/D interface (Digidata 1200, Axon Instruments, Inc., Foster City, CA). The digitized current records were analyzed using a two-threshold transition algorithm that used a 50% threshold-crossing parameter to detect events. The acquisition and analysis of the data were performed with pClamp 6.0 software (Axon Instruments, Inc.).

Channel activity was determined by NP_0 that was calculated as

$$NP_0 = \sum_{n=1}^{N} t_n, \qquad (1)$$

where N is the number of active channels in the patch, P_0 is the open channel probability, and t_n is the fractional open time at each (nth) current level.

For estimating the open probability, P_0, from NP_0 data in some experiments (see e.g., Fig. 2 *B*), we assumed that the total number of channels present in a patch (N) was equal to the maximum number of simultaneous current transitions. However, we should note that this assumption causes an over-estimation of P_0 in low P_0 data. Because the channel activity was quite low (see Fig. 2 *B*), it was not always possible to estimate the number of channels accurately. Therefore, we usually quote NP_0 values for evaluating the activity of the channels present in patches.

To summarize and compare NP_0 data obtained from different patches, NP_0 data in the cytoplasmic Ca^{2+}-sensitivity experiments (see Fig. 3 *B*) were normalized to the value with 100 μM Ca^{2+} in each patch, a concentration in which the channel shows the maximum activity. The voltage dependence of channel activity (see Fig. 2 *C*) was expressed by normalizing the NP_0 value to that obtained at $V_m = -20$ mV. NP_0 data in the ATP (see Figs. 4 and 5), the AMP-PNP analog (see Fig. 6) and the AMP and ADP (see Fig. 7) experiments were also normalized to the control value (no nucleotide) for the same reason.

The normalized NP_0 data in ATP and AMP-PNP experiments were fitted by a competitive inhibition curve described below (see Discussion for detail), using least squares regression analysis.

$$\text{normalized } NP_0 = \frac{NP_{max}}{1 + \dfrac{([X]/K_{d1})^{n1}}{1 + ([X]/K_{d2})^{n2}}}, \qquad (2)$$

where X is ATP or AMP-PNP, NP_{max} is the maximum normalized value of NP_0, K_{d1} and $n1$, and K_{d2} and $n2$ are the dissociation constant and the Hill coefficient of the blocking and relieving effects by X, respectively.

The normalized NP_0 data in ADP experiments were fitted by a single-binding site-inhibition curve described below, using least squares regression analysis.

$$\text{normalized } NP_0 = \frac{NP_{max}}{1 + ([\text{ADP}]/K_{d1})^{n1}}, \qquad (3)$$

where NP_{max} is the maximum normalized value of NP_0, K_{d1} and $n1$ are the dissociation constant and the Hill coefficient of the ADP block, respectively.

Significance of difference between means was determined using Student's paired or unpaired t-test. The level of significance was set at $p \leq 0.05$. All values are expressed as mean ± SE (number of observations).

RESULTS

Basic characteristics of the channel

Figure 1*A* shows single-channel currents recorded from inside-out patches excised from the bullfrog erythrocytes. In these experiments, the cytoplasmic surface of membrane patches was bathed in solutions containing 100 μM Ca^{2+}, and the channel showed brief opening events of 10-ms duration divided by relatively long closed periods of 50–500-ms duration. Occasionally longer closures lasting a few seconds were also observed. We usually did not observe channel activity in cell-attached patches. However, once channel activity appeared after patch excision, the channel maintained a stable activity for more than 20 min or until the giga-seal was broken (without cytoplasmic Mg^{2+} and ATP) and glibenclamide (10–100 μM) failed to suppress channel activity. With a Na^+-rich solution bathing the cytoplasmic face and a K^+-rich solution bathing the extracellular face of the membrane, there was a marked inward rectification of the single-channel currents, and outward currents were not detected. Under these conditions, the reversal potential was more positive than + 40 mV, indi-

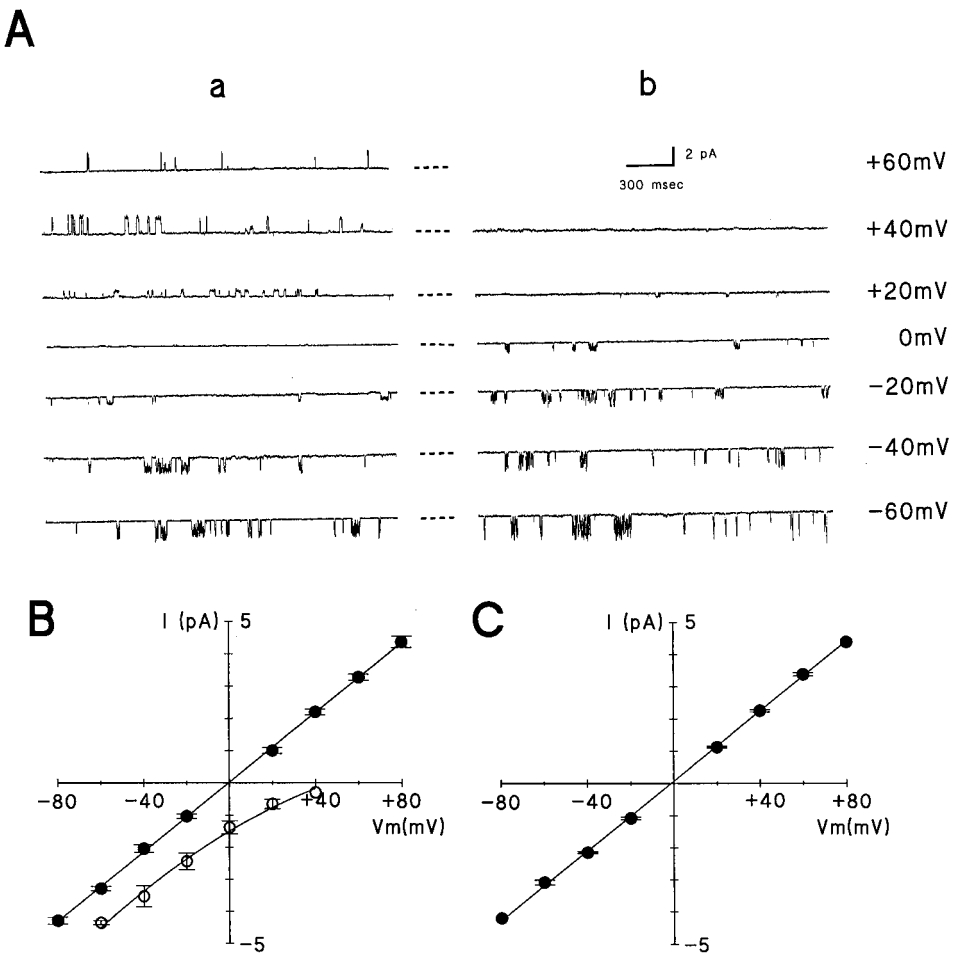

FIGURE 1 Basic characteristics of the ATP-sensitive Ca^{2+}-activated K^+ channel (I). (*A*) Typical single-channel currents recorded from inside-out patches at the membrane potentials (V_m) indicated to the right of each trace. Dashed lines indicate the closed state of the channel. Solutions: (*a*) pipette, K^+-rich; bath, K^+-rich. (*b*) pipette, K^+-rich; bath, Na^+-rich. Bath Ca^{2+} concentration ($[Ca^{2+}]_{bath}$): 100 μM. Low-pass filtered at; 200 Hz. (*B*) Single channel I/V plots. Solutions: (*solid circle*) pipette, K^+-rich; bath, K^+-rich. (*open circle*) pipette, K^+-rich; bath, Na^+-rich. The lines were fit by (*closed circle*) linear and (*open circle*) third-order polynomial least squares regression analysis. (*C*) Effects of Mg^{2+} on single channel I/V relationship. Solutions: pipette, K^+-rich; bath, K^+-rich containing 2 mM Mg^{2+}. The line was fit by linear least square regression analysis.

cating that the channel is predominantly K^+ selective since K^+ is the only ion present with a positive equilibrium potential. When membrane patches were bathed in symmetrical K^+-rich solutions, the I/V relationship was approximately linear and the single-channel conductance was 56 ± 6 pS (n = 6 patches). This is consistent with a previous report of Ca^{2+}-activated K^+ channel of frog erythrocytes (Hamill, 1983). Application of 2 mM $MgCl_2$ to the cytoplasmic face did not significantly affect the I/V relationship (Fig. 1 *C*) or the channel activity (data not shown). This suggests that this channel is not a member of the inward rectifier K^+ channel family (see Nichols and Lopatin, 1997 for review).

The open probability (P_0) of the channels under the same condition, bathed with a saturating cytoplasmic Ca^{2+} concentration (100 μM, see Fig. 3 *B*), varied widely from <0.1 to 0.9 (Fig. 2, *A* and *B*), although most of the channels showed an open probability of < 0.5 (Fig. 2 *B*). Note that the data are presented as P_0, not NP_0. Although P_0 was variable, the single-channel conductance, ion selectivity, and the responses to cytoplasmic Ca^{2+}, ATP, and AMP-PNP were basically the same among the channels with different open-state probability values.

Figure 2 *C* shows the voltage dependence of channel activity at V_m between −80 and +80 mV. When the cytoplasmic face of the membrane was exposed to a saturating Ca^{2+} concentration (100 μM), NP_0 was virtually voltage independent within the range of V_m tested. This poor voltage dependence is consistent with the previous reports of the Ca^{2+}-activated K^+ channel of human erythrocytes (Grygorczyk and Schartz, 1983).

Figure 3 *A* shows single-channel currents recorded from two different inside-out patches at V_m = −20 mV bathed in asymmetrical K^+-rich solutions containing two different bath Ca^{2+} ($[Ca^{2+}]_{bath}$) concentrations. The patch shown in Fig. 3 *A*(*a*) contained channels with high activity, and the patch shown in Fig. 3 *A*(*b*) contained a channel(s) with low activity. Lowering the $[Ca^{2+}]_{bath}$ from 1 to 0.1 μM decreased the activity of these channels with different (i.e., high and low) activities in the same way. With a Ca^{2+}-free bath solution (0 Ca^{2+} plus 2 mM EGTA), no opening events were detected (data not shown). Figure 3 *B* summarizes the dependence of channel activity on the cytoplasmic Ca^{2+} concentration. Channel activity increases with increasing $[Ca^{2+}]_{bath}$ and reaches a maximum level at approximately

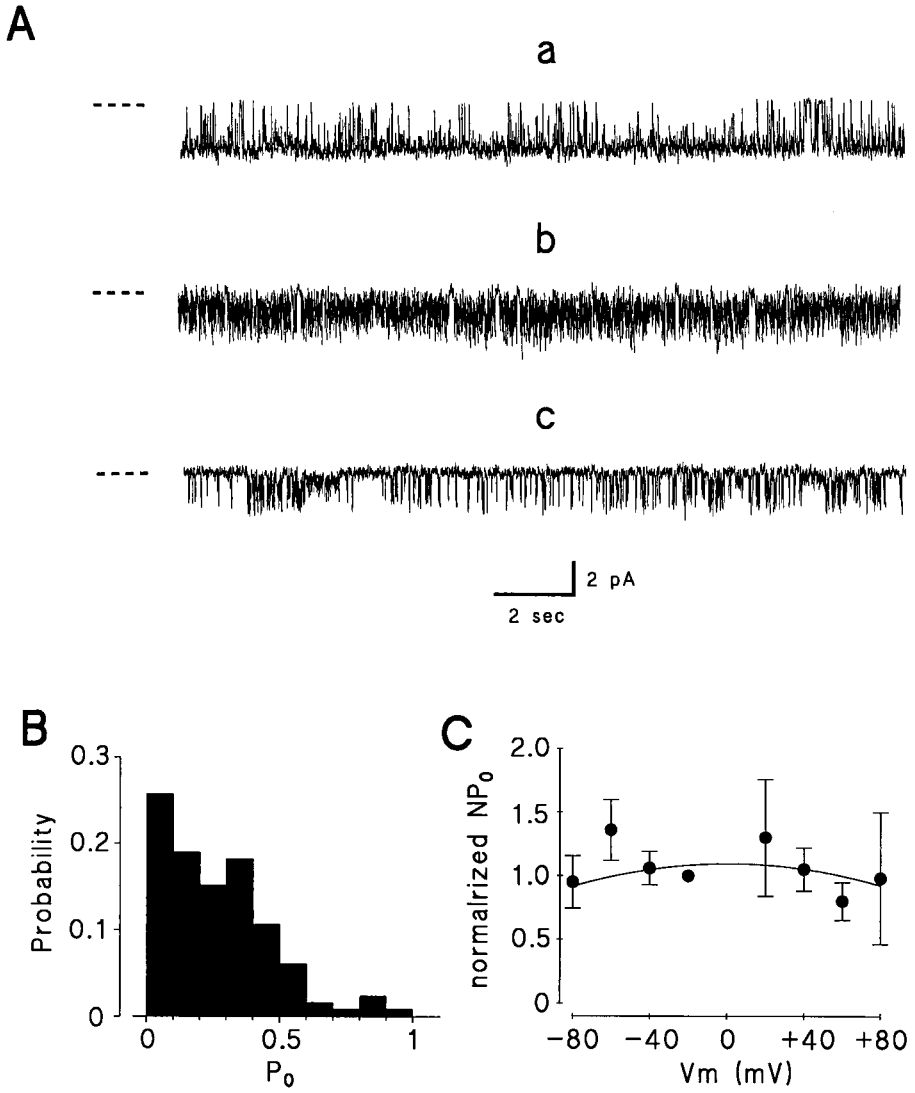

FIGURE 2 Basic characteristics of the ATP-sensitive Ca^{2+}-activated K^+ channel (II). Variation of the channel activity. (*A*) Single-channel currents recorded from three different inside-out patches containing channels showing different channel activity under the same condition. Open probability: (*a*) 0.89; (*b*) 0.30; (*c*) 0.10. Dashed lines indicate the closed state. Solutions: pipette, K^+-rich; bath, Na^+-rich. $[Ca^{2+}]_{bath}$: 100 μM. $V_m = -20$ mV. Low-pass filtered at 200 Hz. (*B*) Distribution of the channel open probability. Ordinate, probability of finding a given open probability (P_0); abscissa, open probability (P_0). Solutions: pipette, K^+-rich; bath, Na^+-rich. $[Ca^{2+}]_{bath}$: 100 μM. $V_m = -20$ mV. Data from 132 patches. (*C*) Effects of membrane potentials on the channel activity. Plots of the normalized NP_0 against membrane potential (V_m). Solutions: pipette, K^+-rich; bath, K^+-rich. $[Ca^{2+}]_{bath}$: 100 μM. Data from 7 patches. Values of NP_0 were normalized by the value at $V_m = -20$ mV. The line was fitted by 2nd-order polynomial least squares regression analysis.

$[Ca^{2+}]_{bath} = 10$ μM with a half maximum value of 600 nM. Note that the channel activity is expressed as NP_0, normalized to the value with 100 μM Ca^{2+}. These results are consistent with previous reports about the Ca^{2+} dependence of the Ca^{2+}-activated K^+ channel of frog erythrocytes (Hamill, 1983) and of human erythrocytes (Grygorcyzk et al., 1984; Leinders et al., 1992a,b).

Taken together, these data demonstrate that this channel is very similar to the intermediate conductance Ca^{2+}-activated K^+ channels previously identified in frogs (*Rana pipiens*) by Hamill (1983), and corresponds to the intermediate conductance Ca^{2+}-activated Gardos K^+ channel in human erythrocytes (Gardos, 1958; Grygorcyzk and Schartz, 1983).

Effects of ATP on single-channel activity

We investigated the effects of cytoplasmic ATP on single-channel activity. For these experiments, we used the Na^+-rich bath solution containing 2 mM $CaCl_2$ and no EGTA to avoid any changes in channel activity caused by a reduction in free Ca^{2+} concentration by ATP-chelation (Kloekner and Isenberg, 1992). It should be also noted that the bath solution was normally Mg^{2+}-free.

Figure 4 *A* shows a continuous single-channel recording obtained from an inside-out patch and the response to the sequential application of 10 μM and 1 mM Na_2ATP to the bath solution. The initial application of 10 μM Na_2ATP to the cytoplasmic face of the patch suppressed channel activity that was fully recovered by washing out the Na_2ATP. However, the application of a higher concentration (1 mM) of Na_2ATP, to the same patch did not affect channel activity significantly (Fig. 4 *A*). Figure 4 *B* shows single-channel data recorded under a faster time base, from an inside-out patch in the presence of 1 mM and 10 μM Na_2ATP sequentially added in the inverted order of Fig. 4 *A*. The initial application of 1 mM Na_2ATP did not affect channel activity significantly, whereas the sequential application of 10 μM

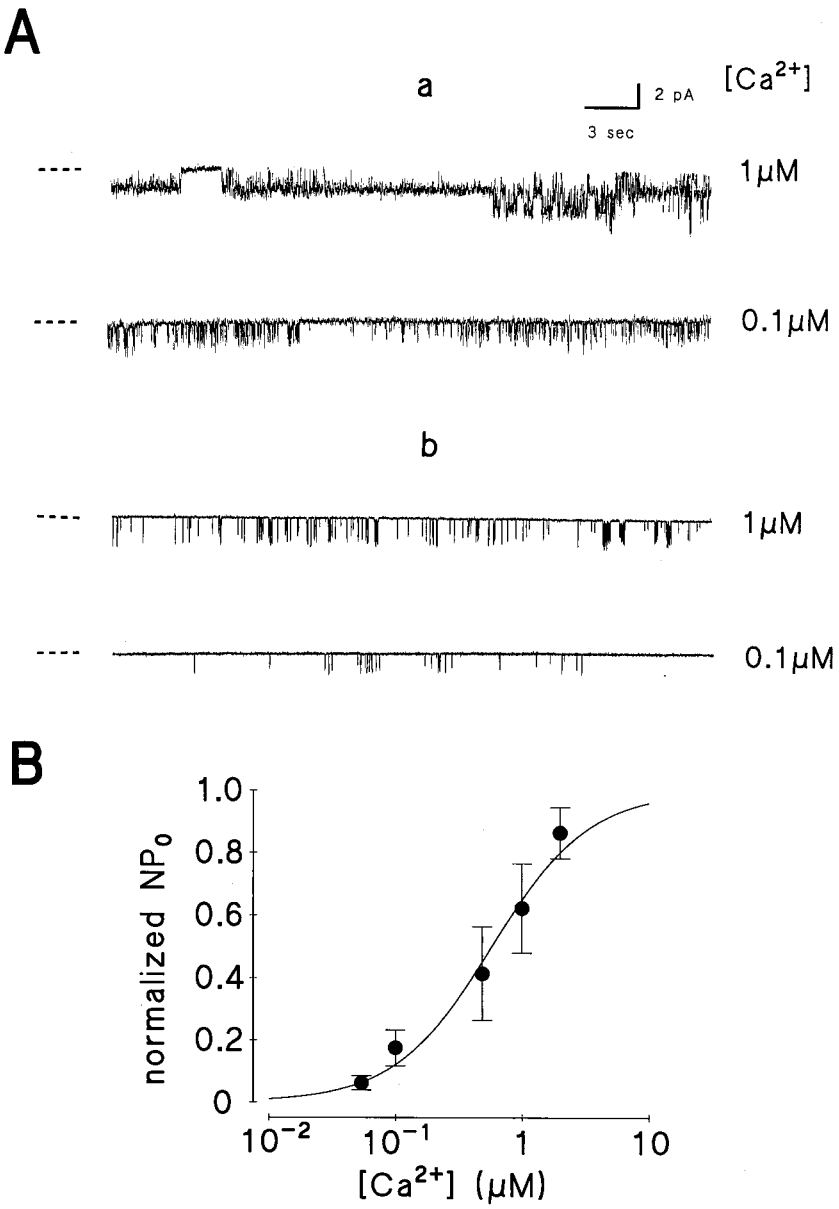

FIGURE 3 Effects of Ca^{2+} concentrations on the channel activity. (*A*) Single-channel currents recorded from two different inside-out patches bathed in asymmetrical K^+-rich solutions containing the indicated Ca^{2+} concentrations in the bath solution. Dashed lines indicate the closed state. NP_0: (*a*) (1 μM) 0.96, (0.1 μM) 0.11; (*b*) (1 μM) 0.043, (0.1 μM) 0.010. Solutions: pipette, K^+-rich; bath, Na^+-rich. $V_m = -20$ mV. Low-pass filtered at 200 Hz. (*B*) Summary of the effects of Ca^{2+} concentrations on the channel activity (normalized NP_0). Solutions: pipette, K^+-rich; bath, Na^+-rich. $V_m = -20$ mV. Data from 8 patches with NP_0 of 0.13–0.96 (0.30 $\pm$ 0.08) with 100 μM Ca^{2+}. Values of NP_0 were normalized by the value with 100 μM Ca^{2+} in each patch. The solid line was best fitted by $NP_0 = 1/\{1 + ([Ca^{2+}]/K_d)^{-n}\}$ with $K_d = 5.8 \times 10^{-7}$ and $n = 1.1$.

Na_2ATP to the same patch suppressed channel activity, which was fully recovered by washing out the Na_2ATP (Fig. 4 *B*). Figure 4 *C* summarizes the effects of Na_2ATP on channel activity. ATP blocked the channel in a biphasic, concentration-dependent manner. ATP dose-dependently inhibited the channel at concentrations <10 μM. However, increasing ATP concentration above 100 μM relieved the ATP block and the nucleotide did not affect channel activity significantly at concentrations >1 mM.

ATP did not cause these effects via Ca^{2+}-chelation, because the free-Ca^{2+} concentration of the bathing solution used in these experiments was always much higher than the Ca^{2+} concentration required for maximum channel activity (100 μM). Moreover, Ca^{2+}-chelation cannot explain the relief of the block at ATP concentrations >100 μM.

We also tested the effects of cytoplasmic ATP on single-channel activity under a physiological Ca^{2+} concentration. Keeping $[Ca^{2+}]_{bath}$ constant at 0.1 μM, ATP blocked the channel in the same way, i.e., application of 10 μM Na_2ATP decreased NP_0 from 0.074 $\pm$ 0.005 (in control) to 0.007 $\pm$ 0.003 (9 $\pm$ 4% of control), whereas application of 1 mM Na_2ATP did not affect channel activity significantly ($NP_0 = 0.073 \pm 0.007$) ($n = 5$ patches).

Effects of PKA/PKC inhibitors on ATP block

We next tested the effects of protein kinase inhibitors on the ATP block. Figure 5 *A* shows typical single-channel current recordings obtained from inside-out patches in response to

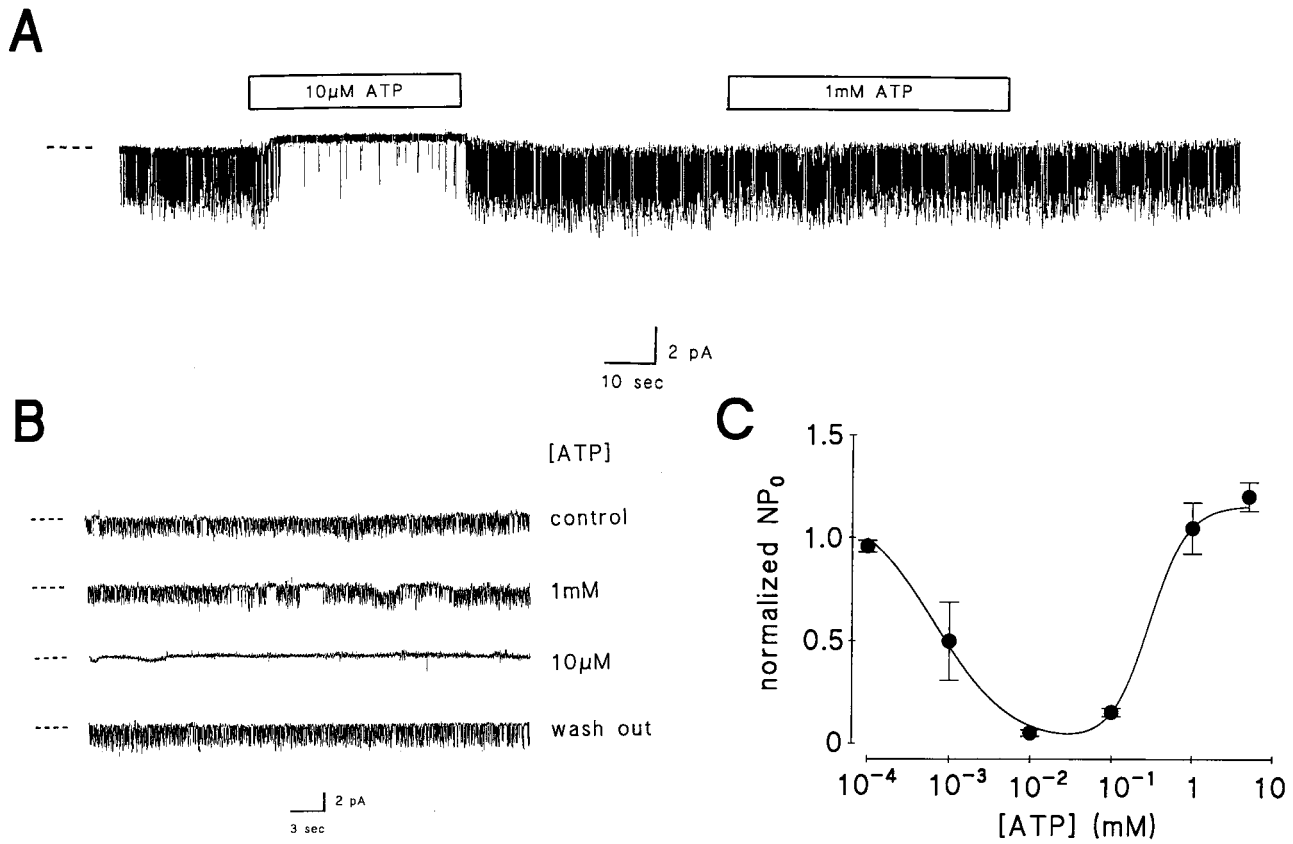

FIGURE 4 Effects of ATP on the channel activity. (*A*) A continuous single-channel recording obtained from an inside-out patch in the sequential application of 10 μM and 1 mM Na_2ATP to the bath solution. Dashed lines indicate the closed state. Solutions: pipette, K^+-rich; bath, Na^+-rich. Bath Ca^{2+} concentration ($[Ca^{2+}]_{bath}$): 2 mM (no EGTA). $V_m = -20$ mV. Low-pass filtered at 200 Hz. (*B*) Typical single-channel current recordings obtained from an inside-out patch in response to 1 mM and 10 μM Na_2ATP, respectively. Dashed lines indicate the closed state. NP_0: (control) 0.27; (1 mM) 0.25; (10 μM) 0.001; (wash out) 0.26. Solutions: pipette, K^+-rich; bath, Na^+-rich. Bath Ca^{2+} concentration ($[Ca^{2+}]_{bath}$): 2 mM (no EGTA). $V_m = -20$ mV. Low-pass filtered at 200 Hz. (*C*) Summary of the effects of Na_2ATP on the channel activity (normalized NP_0). Solutions: pipette, K^+-rich; bath, Na^+-rich. $[Ca^{2+}]_{bath}$: 2 mM (no EGTA). $V_m = -20$ mV. Data from 17 patches with NP_0 of 0.056–0.47 (0.25 $\pm$ 0.03) in control. Values of NP_0 were normalized by the value in control condition in each patch. The solid line was fitted by Eq. 2 with $NP_{max} = 1.2$, $K_{d1} = 0.67$ μM, $n1 = 0.94$, $K_{d2} = 37.2$ μM and $n2 = 2.8$.

Na_2ATP in the presence of a PKA-specific inhibitor, H-89 and a PKC-specific inhibitor, Bisindolylmaleimide I. Neither the PKA inhibitor or PKC inhibitor alone affected channel activity significantly. However, application of 10 μM Na_2ATP suppressed channel activity in a similar manner to that seen in the absence of inhibitor (Fig. 5 *A*, *b* and *d*); in contrast, 1 mM Na_2ATP did not change channel activity (Fig. 5 *A*, *a* and *c*).

Figure 5, *B* and *C*, summarizes the effects of the PKA- and PKC-specific inhibitors on the ATP block, respectively. When compared to control experiments (Fig. 4 *C*), application of the PKA inhibitor or the PKC inhibitor in addition to the Mg^{2+}-free condition (absence of co-substrate), had no significant effect on the ATP block over the whole ATP concentration range tested. This was for both the inhibitory phase of the dose-response, at low ATP concentrations, and the relieving phase at higher ATP concentrations, indicating that protein phosphorylation by PKA or PKC is not involved in the response to ATP.

Effects of AMP-PNP on single-channel activity

Finally we tested the effects of the non-hydrolyzable ATP analog, AMP-PNP, on channel activity. Figure 6 shows single-channel current recordings obtained from an inside-out patch in response to 10 μM and 1 mM AMP-PNP sequentially added to the bath solution. The initial application of 10 μM AMP-PNP to the cytoplasmic face of the patch suppressed channel activity. However, application of a higher concentration (1 mM) of AMP-PNP to the same patch did not suppress channel activity (Fig. 6 *A*). Figure 6 *B* summarizes the effects of the nonhydrolyzable ATP analog on channel activity. AMP-PNP decreased NP_0 in a biphasic manner similar to ATP within a similar concentration range. AMP-PNP maximally inhibited channel activity at a concentration around 10 μM (14 $\pm$ 4% of normalized NP_0 in control), with less inhibition at lower and higher concentrations than 10 μM. We also confirmed that the

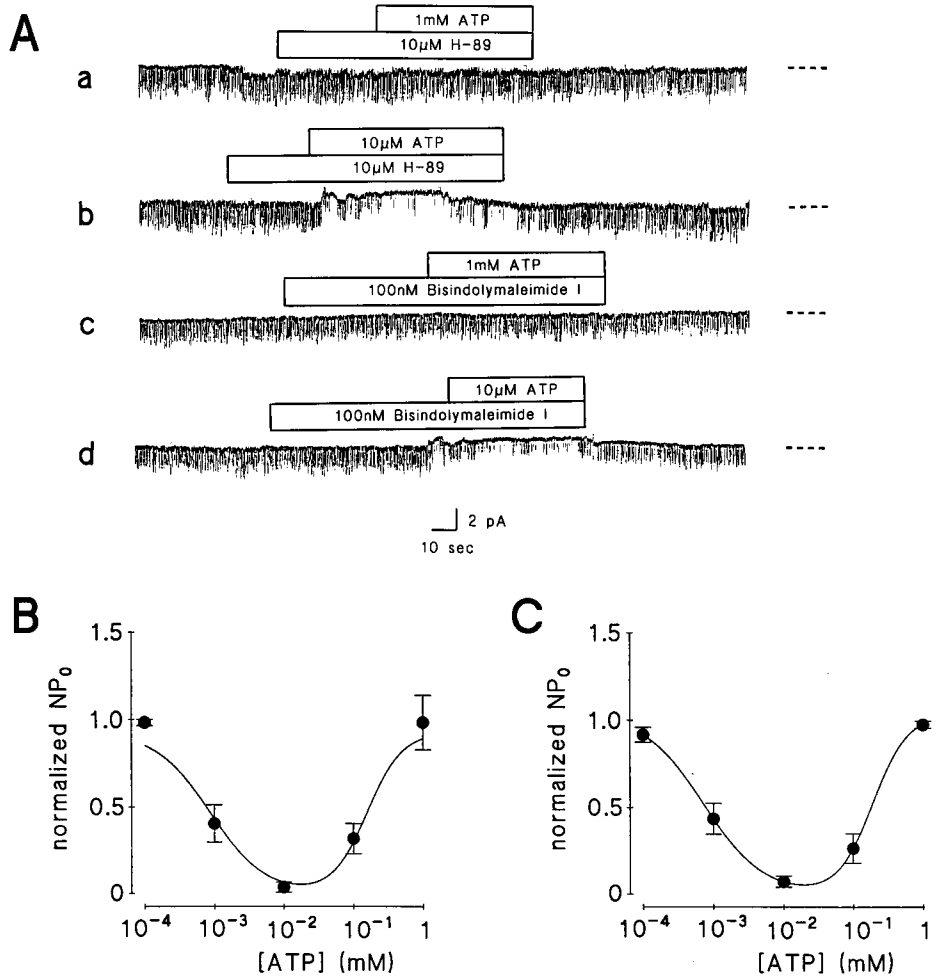

FIGURE 5 Effects of a PKA inhibitor and a PKC inhibitor on the ATP block. (*A*) Typical single-channel current recordings obtained from inside-out patches in response to Na_2ATP under application of (*a*, *b*) a PKA-specific inhibitor, H-89 (10 μM), and (*c*, *d*) a PKC-specific inhibitor, Bisindolylmaleimide I, Hydrochloride (100 nM), respectively. ATP concentrations: (*a*, *c*) 1 mM; (*b*, *d*) 10 μM. Dashed lines indicate the closed state. Solutions: pipette, K^+-rich; bath, Na^+-rich. Bath Ca^{2+} concentration ($[Ca^{2+}]_{bath}$): 2 mM (no EGTA). $V_m = -20$ mV. Low-pass filtered at 200 Hz. (*B*) Summary of the effects of PKA inhibitor, H-89, on the ATP block. Normalized NP_0 under application of 10 μM H-89 and several different concentrations of ATP are shown. Data from 11 patches. Values of NP_0 were normalized by the value in control condition (no ATP, no H-89) in each patch. Solutions: pipette, K^+-rich; bath, Na^+-rich. $[Ca^{2+}]_{bath}$: 2 mM (no EGTA). $V_m = -20$ mV. The solid line was fitted by Eq. 2 with $NP_{max} = 0.93$, $K_{d1} = 0.86$ μM, $n1 = 1.1$, $K_{d2} = 20.4$ μM and $n2 = 2.8$. (*C*) Summary of the effects of PKC inhibitor, Bisindolylmaleimide I, on the ATP block. Normalized NP_0 under application of 100 nM Bisindolylmaleimide I, Hydrochloride and several different concentrations of ATP are shown. Data from 12 patches. Values of NP_0 were normalized by the value in control condition (no ATP, no Bisindolylmaleimide I) in each patch. Solutions: pipette, K^+-rich; bath, Na^+-rich. $[Ca^{2+}]_{bath}$: 2 mM (no EGTA). $V_m = -20$ mV. The solid line was fitted by Eq. 2 with $NP_{max} = 1.0$, $K_{d1} = 0.73$ μM, $n1 = 1.0$, $K_{d2} = 23.7$ μM and $n2 = 2.7$.

presence of Li^+ (we used the lithium salt of AMP-PNP) made little contribution to the effect of AMP-PNP (see Materials and Methods). The effect of AMP-PNP is not caused by possible contaminating ATP, because the activity/concentration curve in the AMP-PNP experiments is shifted ½–1/10-fold in the lower concentration direction when compared to the ATP experiments (compare Fig. 6 *B* with Fig. 4 *B*), whereas the activity/concentration curve in the AMP-PNP experiments would be expected to shift at least 100-fold in the opposite direction, if this were the case. The slight difference in concentration-dependence between AMP-PNP block and ATP block might come from difference in molecular structure between AMP-PNP and ATP.

The fact that the nonhydrolyzable ATP analog could mimic the effect of ATP suggests that ATP affects the channel activity by direct ligand binding and not by phosphorylation of the channel or associated control sites.

Effects of ADP and AMP on single-channel activity

Next we tested the effects of ADP and AMP on channel activity. Figure 7 *A* shows single-channel current recordings obtained from an inside-out patch in response to 1 μM and 1 mM ADP sequentially added to the bath solution. The

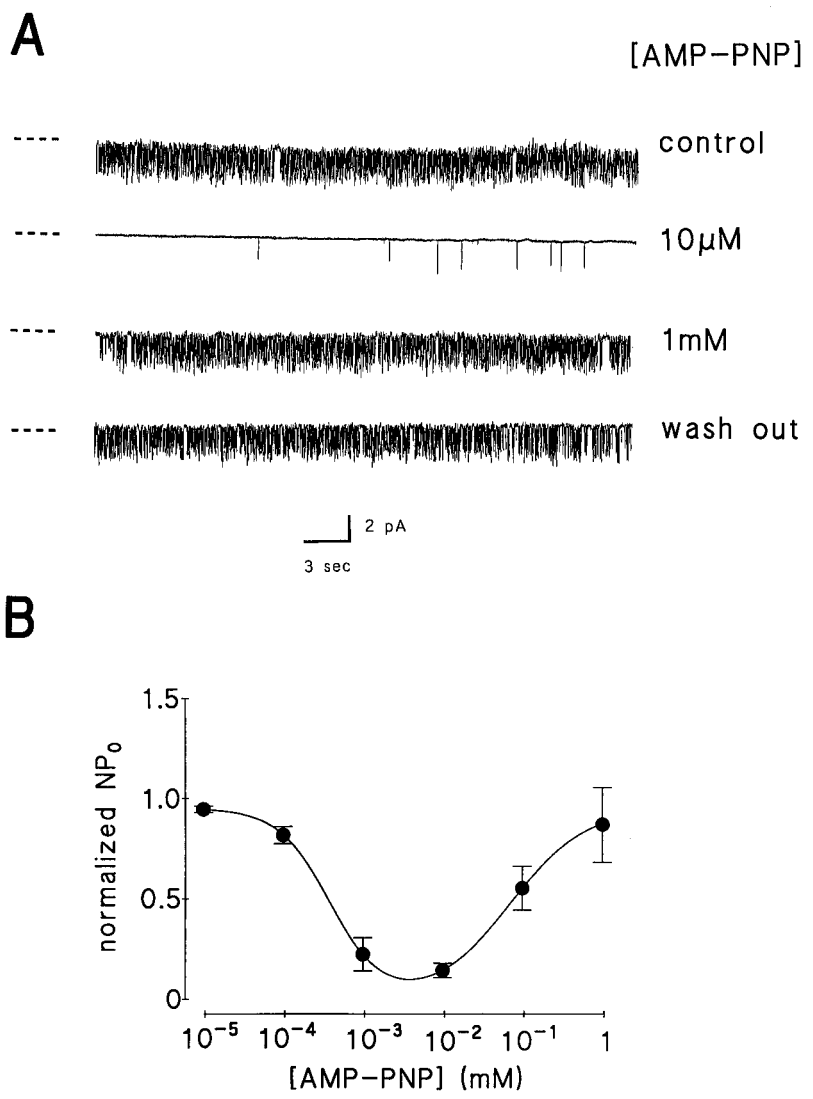

FIGURE 6 Effects of a nonhydrolyzable ATP analog on the channel activity. (*A*) Typical single-channel current recordings obtained from inside-out patches in response to 10 μM and 1 mM AMP-PNP, respectively. Dashed lines indicate the closed state. NP_0: (control) 0.22; (10 μM) 0.001; (1 mM) 0.21; (wash out) 0.22. Solutions: pipette, K^+-rich; bath, Na^+-rich. Bath Ca^{2+} concentration ($[Ca^{2+}]_{bath}$): 2 mM (no EGTA). $V_m = -20$ mV. Low-pass filtered at 200 Hz. (*B*) Summary of the effects of AMP-PNP on the channel activity (normalized NP_0). Solutions: pipette, K^+-rich; bath, Na^+-rich. $[Ca^{2+}]_{bath}$: 2 mM (no EGTA). $V_m = -20$ mV. Data from 11 patches with NP_0 of 0.11–0.65 (0.38 $\pm$ 0.05) in control. Values of NP_0 were normalized by the value in control condition in each patch. The solid line was fitted by Eq. 2 with $NP_{max} = 0.95$, $K_{d1} = 0.37$ μM, $n1 = 1.3$, $K_{d2} = 3.1$ μM and $n2 = 2.3$.

application of Na_2ADP to the patch concentration-dependently suppressed channel activity, which was fully recovered by washing out the Na_2ADP. Figure 7 *B* summarizes the effects of ADP and AMP on channel activity. In contrast to ATP, ADP blocked the channel in a simple concentration-dependent manner with the dose-response giving a $K_d = 71$ nM and a Hill constant of 0.82. AMP had no effect on channel activity over the concentration range 100 nM to 1 mM. The concentration dependence of the ADP block was similar to the inhibitory phase of the ATP block, although the K_d value is one-tenth of that found for the ATP block. However, unlike the ATP response, increasing the concentration of ADP to between 100 μM and 1 mM failed to relieve the block. It should be also noted that application of 1 mM ATP failed to relieve the block induced by 10 μM ADP (five out of five attempts, data not shown). These results suggest that the inhibitory mechanism by adenine nucleotides might involve a binding site that has a higher affinity for ADP than ATP but no significant affinity for AMP.

DISCUSSION

In this report, we have identified an intermediate conductance Ca^{2+}-activated K^+ channel from bullfrog erythrocytes using the patch-clamp technique. With symmetrical K^+-rich (117.5 mM) solutions, the I/V relationship was approximately linear, and the single-channel conductance was 56 $\pm$ 6 pS ($n = 6$). Cytoplasmic Mg^{2+} did not cause inward rectification even at millimolar concentrations. The calcium-sensitivity is higher than the large conductance maxi-K^+ channels, with the calcium concentration causing a half-maximum activation of 600 nM. These basic characteristics are almost identical to the erythrocyte Ca^{2+}-activated K^+ channel identified on frog (Rana *pipiens*) eryth-

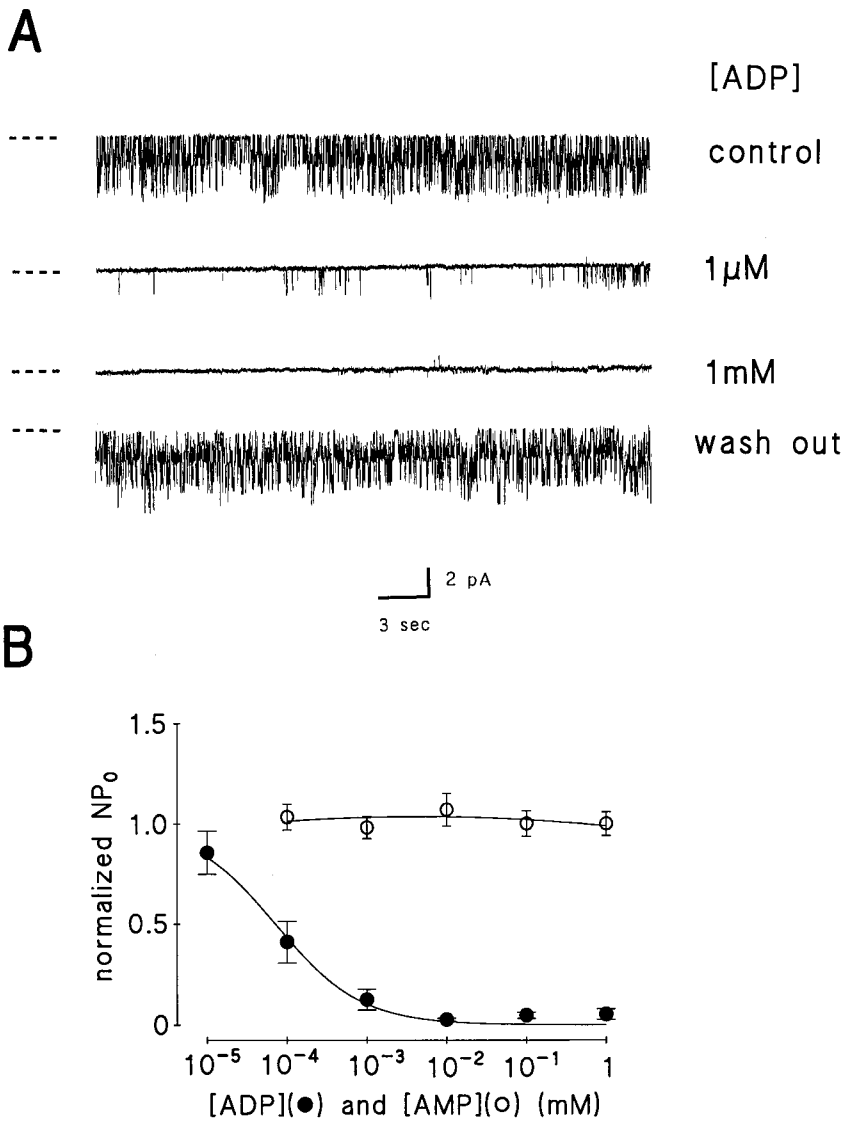

FIGURE 7 Effects of ADP and AMP on the channel activity. (*A*) Typical single-channel current recordings obtained from inside-out patches in response to 1 μM and 1 mM ADP, respectively. Dashed lines indicate the closed state. NP_0: (control) 1.18; (1 μM) 0.016; (1 mM) 0.001; (wash out) 1.14. Solutions: pipette, K^+-rich; bath, Na^+-rich. Bath Ca^{2+} concentration ($[Ca^{2+}]_{bath}$): 2 mM (no EGTA). $V_m = -20$ mV. Low-pass filtered at 200 Hz. (*B*) Summary of the effects of (*closed circle*) ADP and (*open circle*) AMP on the channel activity (normalized NP_0). Solutions: pipette, K^+-rich; bath, Na^+-rich. $[Ca^{2+}]_{bath}$: 2 mM (no EGTA). $V_m = -20$ mV. Data from (ADP) 13 patches with NP_0 of 0.08–0.59 (0.35 $\pm$ 0.04), and (AMP) 13 patches with NP_0 of 0.06–0.52 (0.26 $\pm$ 0.04), in control. Values of NP_0 were normalized by the value in control condition in each patch. The solid line was fitted by Eq. (3) with $NP_{max} = 1$, $K_{d1} = 71$ nM, $n1 = 0.82$.

rocytes (Hamill, 1983) and similar to those of the human Gardos channel (Grygorcyzk and Schartz, 1983). We conclude that the bullfrog erythrocyte Ca^{2+}-activated K^+ channel corresponds to the Gardos channel on human erythrocytes, which has been categorized as an $SK_{(Ca)}$ channel (Latorre et al., 1989; McManus, 1991).

It has been also reported that ATP regulates the activity of several Ca^{2+}-activated K^+ channels via phosphorylation and dephosphorylation of the channel or associated regulatory proteins, and via Ca^{2+}-chelation (see Levitan, 1994; Hilgemann, 1997 for review). We found that cytoplasmic ATP blocked the bullfrog erythrocyte Ca^{2+}-activated K^+ channel in a novel, bell-shaped concentration-dependent manner. Surprisingly, the biphasic ATP block did not require Mg^{2+}, was not dependent on PKA and PKC, and was mimicked by a nonhydrolyzable ATP analog, AMP-PNP. Overall, our results show that ATP directly blocks the channel at low concentrations, and causes a relief of block at high concentrations by binding to sites on the channel or associated control sites.

The direct block by ATP is the specific property of ATP-sensitive K^+ channels (see Ashcroft and Ashcroft, 1990 for review). ATP-sensitive K^+ channels, characterized by inhibition on exposure of the cytoplasmic surface to micromolar to millimolar concentrations of ATP, have been found in a variety of cell types. Ashcroft and Ashcroft (1990) classified ATP-sensitive K^+ channels into five categories based on their sensitivity to ATP, their regulation by intracellular Ca^{2+} and selectivity for K^+, including "type 3," in which the K^+-selective channels were inhibited by ATP and activated by micromolar Ca^{2+}. These type 3, Ca^{2+}-activated, ATP-sensitive K^+ channels have been identified on *Amphiuma* early distal tubule (Hunter and Giebisch, 1988), human nasal polyps (Kunzelmann et al.,

1989), rat neurons (Jiang et al., 1994), and T84 and CFPAC-1 cells (Roch et al., 1995). In terms of the single-channel conductance, the 35-pS inwardly rectifying K^+ channel found in T84 and CFPAC-1 cells (Roch et al., 1995) is the most similar one to the bullfrog erythrocyte Ca^{2+}-activated K^+ channel described here (other type 3 channels have conductance of 200–300 pS). However, ATP blocks these channels in a simple concentration-dependent manner.

The bullfrog erythrocyte Ca^{2+}-activated K^+ channel showed a novel biphasic (inverse bell-shaped) concentration dependence on ATP, in which channel activity was inhibited at low concentrations of ATP, but the block was relieved at high ATP concentrations. Various ATP-sensitive K^+ channels have been reported to also show a biphasic ATP sensitivity, but the concentration dependence of channel activity in these cases is opposite from what we have found (see Ashcroft and Ashcroft, 1990 for review). In these cases, ATP is thought to cause activation at low ATP concentrations by phosphorylation and direct inhibition at high ATP concentrations (Nichols and Lederer, 1991). This is inconsistent with the mechanism of ATP block in the bullfrog erythrocyte Ca^{2+}-activated K^+ channels.

A possible model of the ATP block

As discussed above, the biphasic response of channel activity to ATP is thought to be caused by a direct ligand-binding mechanism. Channel activity at high (millimolar) ATP concentrations reaches approximately the same level as the control experiments (normalized $NP_0 = 1$). Moreover, the effects of ADP (Fig. 7) suggested that the channel had an independent binding site for blocking the channel.

To explain the biphasic ATP block, we propose a "competitive inhibition" model that has two different ATP binding sites; a blocking site, which, with ATP bound, leads to channel block, and a relieving site, which, when ATP is bound, prevents ATP binding to the blocking site. The affinity of ATP for the blocking site ($K_d = \sim 0.7\ \mu M$) is much higher than that for the relieving site ($K_d = \sim 40\ \mu M$). The Hill coefficient of ATP binding to the blocking and the relieving sites are 0.94 and 2.8, respectively (Fig. 4). Therefore, as a simple interpretation (Fig. 8), over the ATP concentration range lower than 10 μM, the channel is blocked by a single ATP molecule binding to the blocking site, whereas, at ATP concentrations higher than 100 μM, three ATP molecules bind to the relieving site and prevent ATP binding to the blocking site, perhaps via a conformational change of the blocking site. The blocking site also has a 10-fold higher affinity for ADP than for ATP, however, the relieving site does not have a significant affinity for ADP (Fig. 7). Both binding sites have no significant affinity for AMP (Fig. 7) whereas AMP-PNP binds to each site with a slightly different affinity than ATP (Fig. 6). The failure of 1 mM ATP to relieve the block induced by 10 μM ADP (data not shown) does not exclude the competitive inhibition model, although it may indicate that the model is not complete.

We cannot exclude some other possible models, e.g., a two-independent (blocker and activator) site model or a substrate inhibition model. However, we believe a two-independent site model is unlikely because channel activity (NP_0) reaches approximately the same level at high (millimolar) ATP concentration as the initial control value (in the absence of ATP). Because control NP_0 values varied widely in our experiments (NP_0: 0.06–0.5, see Fig. 4 *C*), it would seem more likely that, at high ATP concentration, when the activator site would be fully occupied, we would expect the NP_0 values to be several-fold higher than the original control values, especially in channels with low activity, but this was not the case.

In the substrate inhibition model, it is very unlikely that the substrate inhibits the effects of the same substrate completely, even at high substrate concentrations. Therefore, both models are less likely than the competitive inhibition model.

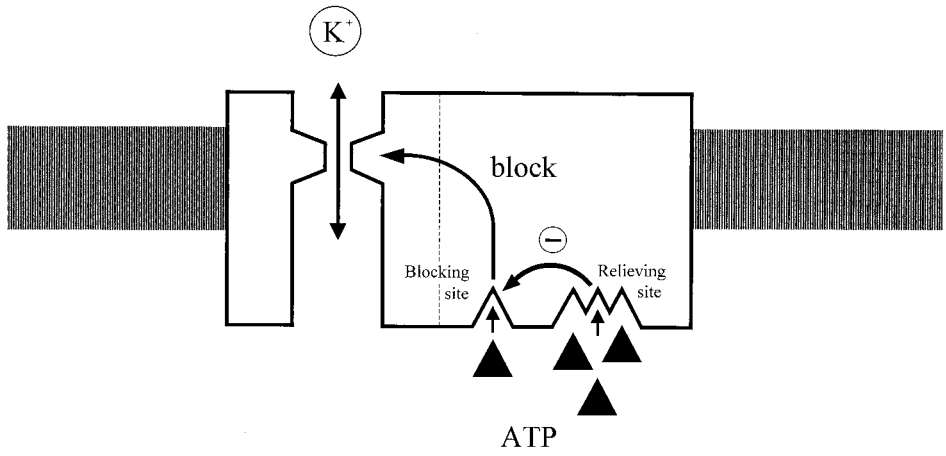

FIGURE 8 A depiction of a possible model of the ATP block on the intermediate conductance Ca^{2+}-activated K^+ channel on bullfrog erythrocytes. See text for detail.

The physiological role of this K^+ channel is still unclear. However, because its basic characteristics are comparable to those of the Gardos channel, it is speculated that this channel might play a role in the regulation of cell volume and ion content in the erythrocyte (see Brugnara, 1997 for review).

In conclusion, we have identified an intermediate conductance Ca^{2+}-activated K^+ channel on bullfrog erythrocytes, which is blocked by ATP in a novel, biphasic (bell-shaped) concentration-dependent manner probably by direct ligand binding of ATP to the channel protein or associated regulatory proteins.

We thank Dr. M. A. Gray for critically reading the manuscript.

This work was supported by a grant-in-Aid for Scientific Research from the Ministry of Education, Science, Sports, and Culture of Japan (07770040) to Y.S.

REFERENCES

Ashcroft, S. J. H., and F. M. Ashcroft. 1990. Properties and functions of ATP-sensitive K-channels. *Cell. Signalling.* 2:197–214.

Brugnara, C. 1997. Erythrocyte membrane transport physiology. *Curr. Opin. Hematol.* 4:122–127.

Christophersen, P. 1991. Ca^{2+}-activated K^+ channel from human erythrocyte membranes: single channel rectification and selectivity. *J. Membr. Biol.* 119:75–83.

Gardos, G. 1958. The function of calcium in the potassium permeability of human erythrocytes. *Biochim. Biophys. Acta.* 30:653–654.

Grygorcyzk, R., and W. Schartz. 1983. Properties of the Ca^{2+}-activated K^+ conductance of human red cells as revealed by the patch-clamp technique. *Cell Calcium.* 4:499–510.

Grygorcyzk, R., W. Schartz, and H. Passow. 1984. Ca^{2+}-activated K^+ channels in human red cells. Comparison of single-channel currents with ion fluxes. *Biophys. J.* 45:693–698.

Hamill, O. P. 1983. Potassium and chloride channels in red blood cells. *In* Single Channel Recording. B. Sakmann and E. Neher, editors. Plenum Publishing Corp., New York. 191–263

Hilgemann, D. W. 1997. Cytoplasmic ATP-dependent regulation of ion transporters and channels: mechanisms and messengers. *Annu. Rev. Physiol.* 59:193–220.

Hunter, M., and G. Giebisch. 1988. Calcium-activated K-channels of *Amphiuma* early distal tubule: inhibition by ATP. *Pfluegers Arch.* 412: 331–333.

Jiang, C., F. J. Sigworth, and G. G. Haddad. 1994. Oxygen deprivation activates an ATP-inhibitable K^+ channel in substantia nigra neurons. *J. Neurosci.* 14:5590–5602.

Kloekner, U., and G. Isenberg. 1992. ATP suppresses activity of Ca^{2+}-activated K^+ channels by Ca^{2+} chelation. *Pfluegers Arch.* 420:101–105.

Kunzelmann, K., H. Pavenstadt, and R. Greger. 1989. Characterization of potassium channels in respiratory cells. II. Inhibitors and regulation. *Pfluegers Arch.* 414:297–303.

Latorre, R., A. Oberhauser, P. Labarca, and O. Alvarez. 1989. Varieties of calcium-activated potassium channels. *Annu. Rev. Physiol.* 51:385–399.

Levitan, I. B. 1994. Modulation of ion channels by protein phosphorylation and dephosphorylation. *Annu. Rev. Physiol.* 56:193–212.

Leinders, T., R. G. D. M. Van Kleef, and H. P. M. Vijverberg. 1992a. Single Ca^{2+}-activated K^+ channels in human erythrocytes: Ca^{2+} dependence of opening frequency but not of open life time. *Biochim. Biophys. Acta.* 1112:67–74.

Leinders, T., R. G. D. M. Van Kleef, and H. P. M. Vijverberg. 1992b. Distinct metal ion binding sites on Ca^{2+}-activated K^+ channels in inside-out patches of human erythrocytes. *Biochim. Biophys. Acta.* 1112: 75–82.

McManus, O. B. 1991. Calcium-activated potassium channels: regulation by calcium. *J. Bioenerg. Biomembr.* 23:537–560.

Nichols, C. G., and W. J. Lederer. 1991. The mechanism of K_{ATP} channel inhibition by ATP. *J. Gen. Physiol.* 97:1095–1098.

Nichols, C. G., and A. N. Lopatin. 1997. Inward rectifier potassium channels. *Annu. Rev. Physiol.* 59:171–191.

Roch, I., I. Baro, A. S. Hongre, and D. Escande. 1995. ATP-sensitive K^+ channels regulated by intracellular Ca^{2+} and phosphorylation in normal (T84) and cystic fibrosis (CFPAC-1) epithelial cells. *Pfluegers Arch.* 426:355–363.

Romero, P. J., C. E. Oritz, and C. Militto. 1990. Metabolic control of the K^+ channel of human red cells. *J. Membr. Biol.* 116:19–29.

Romero, P. J., and L. Rojas. 1992. The effect of ATP on $Ca^{(2+)}$-dependent K^+ channels of human red cells. *Acta Cient. Venez.* 43:19–25.

Sohma, Y., A. Harris, B. E. Argent, and M. A. Gray. 1996. Two barium binding sites on a maxi-K^+ channel from human vas deferens epithelial cells. *Biophys. J.* 70:1316–1325.

Sohma, Y., A. Harris, B. E. Argent, and M. A. Gray. 1998. A novel type of internal barium block of a maxi K^+ channel from human vas deferens epithelial cells. *Biophys. J.* 74:199–209.

Toro, L., and E. Stefani. 1991. Calcium-activated potassium channels: metabolic regulation. *J. Bioenerg. Biomembr.* 23:561–576.